



HAL
open science

Impact of photovoltaic power plants on far-field effects of UVCEs

Guillaume Lecocq, Antoine Dutertre, Emmanuel Leprette

► **To cite this version:**

Guillaume Lecocq, Antoine Dutertre, Emmanuel Leprette. Impact of photovoltaic power plants on far-field effects of UVCEs. 13th International symposium on hazards, prevention, and mitigation of industrial explosions (ISHPMIE 2020), Jul 2020, Braunschweig, Germany. pp.284-294, 10.7795/810.20200724 . ineris-03319941

HAL Id: ineris-03319941

<https://ineris.hal.science/ineris-03319941>

Submitted on 13 Aug 2021

HAL is a multi-disciplinary open access archive for the deposit and dissemination of scientific research documents, whether they are published or not. The documents may come from teaching and research institutions in France or abroad, or from public or private research centers.

L'archive ouverte pluridisciplinaire **HAL**, est destinée au dépôt et à la diffusion de documents scientifiques de niveau recherche, publiés ou non, émanant des établissements d'enseignement et de recherche français ou étrangers, des laboratoires publics ou privés.

Impact of photovoltaic power plants on far-field effects of UVCEs

Guillaume Lecocq ^a, Antoine Dutertre ^b & Emmanuel Leprette ^a

E-mail: guillaume.lecocq@ineris.fr

^a Institut National de l'Environnement Industriel et des Risques, Parc Technologique ALATA, BP 2, 60550 Verneuil-en-Halatte, France

^b TOTAL S.A., 2 place Jean Millier, La Défense 6, 92400 Courbevoie, France

Abstract

Photovoltaic power stations are developing worldwide as they emit no greenhouse gases while producing electricity. In France, industries such as Total plan to install such stations in fields surrounding their chemical and refining plants. The risk analyses performed for these plants often highlighted Unconfined Vapor Cloud Explosions scenarios, related to heavy gases releases, for which characteristic overpressure effect distances were computed

The present work aims at quantifying the impact of the presence of a photovoltaic power station in a potential flammable cloud. It is nevertheless limited to a station geometry provided by Total.

The problem is not straightforward as two main physical trends appear: flame acceleration due to panels obstruction and flame extinction when the flame reaches the top of the flammable cloud. It has first to be determined if explosion runaway is possible, this one due to the obstacles repetition on the flame path. Then, characteristic overpressure effects distances can be computed for photovoltaic power plants of any size.

To this goal, a CFD-based method is proposed and detailed. The open-source CFD code OpenFoam is used as well as phenomenological considerations for computing characteristic overpressure effects distances.

Keywords: *photovoltaic power plants, premixed gaseous flame propagation, overpressure effects distances, CFD*

1. Introduction

Some industries such as Total own large lands surrounding their production plants such as refineries. They are often unused and free of any building and therefore perfect candidates for installing photovoltaic power plants. For some of these, scenarios of Unconfined Vapor Cloud Explosions (UVCE) were identified during risk analyses. This kind of phenomenon is related to the potential release of flammable products followed by an ignition of the generated flammable cloud. In the French regulation, the UVCE overpressure effects are quantified by the distances at which the characteristic thresholds of 200, 140, 50 mbar are reached. These distances give regulatory perimeters which constrain land-use planning. Installing photovoltaic power plants requires to check if the pre-existing overpressure effects distances would be significantly modified by the presence of rows of panels in the flammable cloud.

A study co-funded by Total and INERIS was carried out in order to develop a method for quantifying overpressure effects related to the explosion of a flammable cloud covering photovoltaic panels representative of the ones that could be installed by Total around its production plants. This partnership enabled INERIS to gain expertise for modelling dangerous phenomena appearing with

the development of photovoltaic power plants and Total to develop a philosophy for their safe positioning. The paper details some elements of the study.

2. Scenario and problem description

Scenarios of massive releases of heavy hydrocarbons such as propane or equivalent medium reactivity gases could be identified for industrial plants. Due to buoyancy effects, such products when mixed with air generate “flat” flammable clouds *ie* with a maximum height about 3-4 m and a length in order of hundreds of meters. The flammable cloud size is limited by the iso-surface with a concentration that equals the lower flammability limit.

Current projects plan the installation of photovoltaic power plants around some industrial plants. A design example was supplied by Total and is shown in the Figure below. In this case, a rotation of the panels is possible. For this work, two bounding cases were considered: parallel to the ground or inclined with an angle of 45° as in Fig. 1. The panels width and the distance between the rotation point and the ground are about a few meters. A few meters also separate the panels rows.

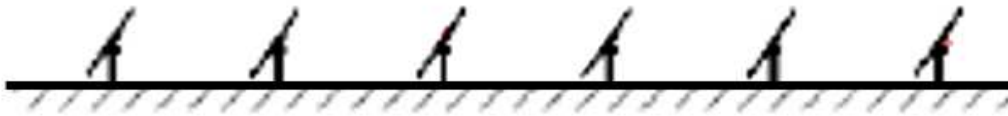


Fig. 1. Cross-section of a photovoltaic power plant designed by Total

The explosion scenario deals with a flammable cloud that can theoretically cover dozens of rows of panels at full height. Before any modelling, the regarded phenomenology should be analysed.

According to experimental works, flat flammable clouds generate slow flames (*ie* the flame speed is about a few m/s) when there is no obstruction in the flammable zone (Zeeuwen, 1983). Furthermore, according to theoretical works (Daubech, 2016), two explosion phases should be distinguished in the case of an ignition source in the flammable zone: a spherical or hemispherical phase during which the burnt gases expansion contributes to the flame propagation followed by an azimuthal phase during which this effect is lost. Two theoretical expressions were derived from the work of Daubech et al. for quantifying the far-field pressure generated by each phase. In the case of flames with a constant speed, they write:

$$\text{Eq. (1)} \quad \Delta p(r, t) \approx \rho_{atm} \frac{4H}{r} \tau(\tau - 1)V_f^2$$

$$\text{Eq. (2)} \quad \Delta p(r, t) \approx \rho_{atm} \frac{2H}{r} (\tau - 1)V_f^2$$

ρ_{atm} is the atmospheric volume mass, H is the flammable cloud height, τ is the burnt gases expansion rate and V_f is the constant flame speed. This set of equations highlights that far from the flame the azimuthal phase pressure is about 2τ times lower than the hemispherical phase pressure.

If there are repeated obstacles in the flat cloud, it can be questioned if the relative importance of each phase in the pressure generation process is kept. In case of ignition in the power plant covered with a flammable cloud, the flame is first spherical, then interacts with the closest panel or panels leading to a distortion which is prone to increase the burned gases production rate. The flame at a given moment reaches the lower flammable concentration at the top of the cloud and a part of the flame front quenches. This latter phenomenon induces a progressive venting of the burnt gases which contributes to slow down the flame whereas in the same time, the flame keeps on propagating in the direction parallel to the ground. During the propagation across the rows of panels, there is a permanent competition between an increase in pressure generation due to flame distortion and venting due to a flame reaching the flammable cloud limits.

Previous experiments showed the separation distance between obstacles could be a key parameter for pressure effects (Van der Berg, 2005). If the obstacles are too close, there can be a continuous acceleration from an obstacle to another leading to a runaway phenomenon. The maximum overpressure in the flammable cloud is then limited by the acceleration length for the flame *ie* the minimum length between the flammable cloud length and the photovoltaic power plant length. Both of them being about hundreds of meters, an explosion runaway cannot be excluded theoretically on this basis.

A practical consequence of the occurrence of such a phenomenon when quantifying the regulation overpressure effects distances is to account for all the flammable mass of the cloud and to assume maximum overpressure in the cloud about several bars. Such assumptions could lead to large overpressure effect distances and restrict the installation of photovoltaic plants.

A method has to be proposed to study the runaway risk and to quantify the regulation effects distances. In the current paper, a modelling approach was chosen.

3. A method mixing CFD and phenomenology

Modelling tools such as the CFD software FLACS (Hansen, 2010) were developed for addressing complex set-ups at the industrial scale. In short, it relies on a URANS approach for modelling turbulence and obstacles are partly resolved by the mesh. A sub-grid porosity accounts for unresolved obstacles. This porosity as well as other physical parameters were calibrated against a large number of explosion trials involving obstacles at large-scale.

This tool was first employed to get a first guess of the pressure effects related to a UVCE developing in a photovoltaic power plant. The related computations did not highlight a global flame acceleration phenomenon. The computed overpressure levels were not significant as they were lower than 20 mbar, except in a few points of the geometry. These punctual peaks dissipated in a few meters and had no effect on the global pressure field.

In order to confirm these results, another approach based on CFD is proposed for modelling a potential explosion in the photovoltaic power plant. For studying the risk of explosion runaway, there must be a few rows of photovoltaic panels in the computational domain whose topology should ideally be 3D. The computational domain has to be a few dozens of meters long in each direction. This first aspect is of importance as computation resources are limited. They will limit the minimum size of the cells of the mesh.

At the moment, it may appear tricky to choose a relevant set of physical sub-models when using CFD to account for large-scale explosions mechanisms. Even an explosion in a flat flame is complex as the following physical effects may appear: interaction of the flame with the wind, self-acceleration due to instabilities more or less pronounced with the fuel and local equivalence ratio and partly explained by non-unitary Lewis number and Markstein length effects. The latter physics requires a mesh fine enough to get a realistic flame thickness and a description of differential diffusion of species and temperature.

Adding obstacles in the cloud, other physical phenomena appear and have to be accounted for, especially if the solar panels rows are inclined: a Karman vortex street in the wake of obstacles, with a characteristic Reynolds number increasing as the flame approaches obstacles, an acceleration of the flame and the fresh gases in front of it between the ground and the bottom of the panels.

Concerning turbulence modelling, Large-Eddy Simulations are attractive as they tend to become the state-of-the-art for engineering problems and get more and more precise as the mesh is refined, limiting the modelled part. Nevertheless, the validity of sub-grid scale models for turbulence and flame/turbulence could be questioned for cells with a characteristic width of a dozens of centimeters. In engineering computations, the characteristic cell width is lower than a millimeter. Furthermore, even well-resolved middle-scale explosions showed a pressure field depending on the chosen turbulent/flame SGS model (Di Sarli, 2010, Quillatre, 2014). URANS modelling works were

proposed for modelling a methane flame acceleration (Lecocq, 2019) in a 24-m long tube but there is no guarantee all the chosen parameters could be re-used at larger scale with a global 3D topology flame.

A modelling method grounded on CFD and phenomenological considerations is proposed and tested in what follows.

a. Modeling method

The current work does not deal with the flammable product dispersion and the flammable cloud generation. It focuses on the explosion stage only.

The 3D flame propagation is modelled with a CFD approach. The transport equations of pressure, momentum, energy, chemical species and progress variable are solved numerically by the OpenFoam code (Weller, 1998), version 5. The solver is compressible. The chemistry is addressed with a one-step reaction and only propane, oxygen, nitrogen, carbon dioxide and water mass fractions are transported. There is no turbulence model. The modelling mainly aims at obtaining a conservative wrinkling factor for the flame during its propagation.

A turbulent premixed flame can be modelled with a flame surface-density ($\bar{\Sigma}$) approach. This quantity is approximated as $\Xi|\nabla c|$, where Ξ is the wrinkling factor of the flame related to an increase of the un-resolved part of the flame surface and c is the progress variable. The chemical source terms appearing in the transport equations of the progress variable and chemical species mass fractions can be closed as (Lecocq, 2011):

$$\text{Eq. (3)} \quad \rho\omega_c = \rho_u S_L \Xi |\nabla c|$$

$$\text{Eq. (4)} \quad \rho\dot{\omega}_{Y_i} = \rho\omega_c (Y_i^b - Y_i^u)$$

Where ρ_u is the volume mass of the fresh gases, S_L is the laminar flame speed, Y_i^b (resp. Y_i^u) is the burnt (resp. fresh) gases mass fraction of the i^{th} chemical species.

This model does not include differential diffusion between temperature and chemical species. If Ξ is set to 1, in case of ignition in a flammable medium at rest with an homogenous concentration, the model accounts for a spherical flame that propagates at a speed: burnt gases expansion rate times the laminar flame speed. Some un-resolved phenomena at grid scale can be included through modifications of the wrinkling factor.

According to some works (Daubech, 2016), a spherical flame propagation without obstacles can be analytically described. The flame speed V_{disf} can write as:

$$\text{Eq. (5)} \quad V_{disf} = \tau V_f = \tau S_L \Xi_{\text{Total}}$$

Where τ is the burnt gases expansion rate and Ξ_{Total} is the wrinkling related to the wind and intrinsic flame instabilities. This latter wrinkling factor was written as: $\Xi_{\text{Total}} = \Xi_I \Xi_{\text{TW}}$ with Ξ_I the wrinkling related to instabilities solely and Ξ_{TW} the wrinkling related to the turbulence of the wind solely. This choice is cautious as recent works have shown at lab scale that depending of the flame position in the theoretical combustion diagram an effect was dominant on the other but there was no combination of the effects (Yang, 2018). For a propane flame, the asymptotic value of Ξ_I and predicted by theory, depends only on the burnt gases expansion rate and is about 3.5. The wind effect is computed with the Gülder correlation (Gülder, 1995) and an integral length scale for the atmospheric turbulence about 1 m and a fluctuating speed about 0.5 m leading to a value of 8 for Ξ_{TW} . Adding all these contributions, mathematically speaking by multiplying the wrinkling factors, the theoretical flame speed during the hemispherical phase of flame propagation is about 90 m/s.

Recent experimental works (Bauwens, 2015) gave for a stoichiometric spherical propane/air flame propagating on a length about 1 m, in a medium initially at rest, an increase of flame surface about 1.5 explained by Darrieus-Landau instabilities. In the target computation, the flame is interacting with photovoltaic panels roughly one meter after ignition. In order not to be too much conservative and

avoid artificial explosion runaway, in the following, Ξ_1 is set to 1.5. The reference propane/air flame propagates at speed of 45 m/s when undergoing burnt gases expansion effects and 6 m/s when it is no longer the case. A case with propylene gives a minimum flame speed of 55 m/s and 7 m/s. The flame speeds for the spherical phases have the same order of magnitude as encountered with the propagation of a spherical stoichiometric hydrogen/air flame (Schneider, 1983) without wind effects. They are one order of magnitude greater than the ones measured in a propane/air explosion free of obstacles. Both observations mean the computed flame speeds remain conservative.

b. First tests

Free fields tests were performed with CFD in a 3D computational domain with 15 cm wide cells in the zone of interest (measured flame and pressure wave propagation). A flammable cloud at rest with a homogenous propane/air concentration was initialized, the height of the cloud being 4 m, the half-length of the cloud being 20 m. The wrinkling factor was tuned to get a minimum flame speed of 72 m/s during hemispherical phase. The computation was redone with another mesh made of 10 cm wide cells in the interest zone.

The results in terms of overpressure at ignition point and 30 m away, out of the flammable cloud are shown in Fig. 2. It can be seen that the same hemispherical phase is predicted at ignition point by both computations. Out of the flammable cloud, the same maximum overpressure is recovered. It means the wave propagation is weakly impacted by the mesh resolution. The azimuthal phase is nevertheless different in both cases: the maximum overpressure at ignition point is about 65 % higher with the fine mesh. Out of the flammable cloud, the same gap is retrieved. This difference between the two meshes is explained by a higher resolved flame wrinkling during the transition between the spherical and the azimuthal phase (Fig. 2b). It is explained by a limit of the proposed CFD model: the added wrinkling factor does not depend on the mesh size whereas if the mesh is refined, more wrinkling appears at the resolved level.

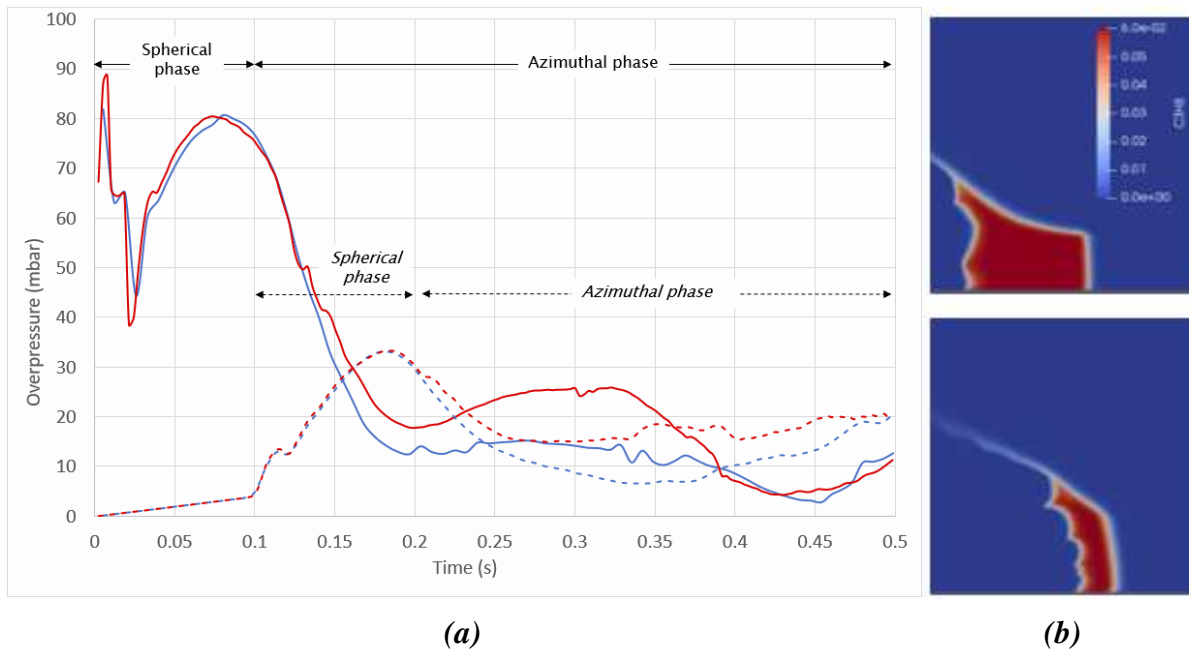


Fig. 2. a) Computed pressure signals at ignition point (line) and 30 m from ignition point (dash line). Blue: reference mesh. Red: fine mesh. **b)** Propane mass fraction contours 300 ms after ignition. Top: reference mesh, bottom: fine mesh.

The overpressure values can be compared with the theory. According to (Lannoy, 1989), for a constant flame speed flame with a flame speed lower than 120 m/s, overpressure in the burnt gases writes:

$$\text{Eq. (6)} \quad \Delta p = \rho_{atm} \left(1 - \frac{1}{\tau}\right) (\tau V_f)^2 \frac{1}{2} \left(3 - \frac{1}{\tau}\right)$$

For a flame propagating at 72 m/s, Eq. (6) gives 78 mbar whereas a value of 80 mbar was obtained with CFD. Eqs. (1) and (2) can be used to predict the overpressure field out of the flammable cloud. For a constant flame speed of 72 m/s (resp 9 m/s) during the hemispherical (azimuthal) flame propagation, 30 m away from ignition point, the maximum overpressure is 14 mbar (resp. 1 mbar). Both CFD computations predict larger values: the overestimation is about 100 % for the hemispherical phase and one order of magnitude for the azimuthal phase. The computation performed with a reference mesh being conservative when compared with theory, it is kept for the computations with a photovoltaic power plant.

4. CFD computations with a photovoltaic power plant

a. Parametric tests

The reference situation is the one of a stoichiometric propane/air cloud at rest covering the photovoltaic panels. Several parameters were of interest: the orientation of the photovoltaic panels (parallel to the ground or inclined), the separation distance between two rows, the height of the cloud and the reactivity of the cloud (propane/air or propylene/air mixture). The computations to be performed to investigate some trends are numerous. It was chosen to perform these computations with an assumption of a 2D-symmetry for a flame propagating perpendicularly to the rows. It implicitly means the flame is cylindrical and the width of the panels is infinite.

The cell width in these computations is 3 cm. When comparing the burnt gases pressure for a given flame speed with theory, the overestimation of the 2D mesh is about 100 %. The computations that follow give overpressures exceeding real ones but enable to identify the main trends, changing a parameter at a time. The criterion between two computations is the overpressure out of the flame. The Fig. 3 details through a zoom on the computational domain the location of main pressure probes relative to the flammable cloud and the photovoltaic panels.

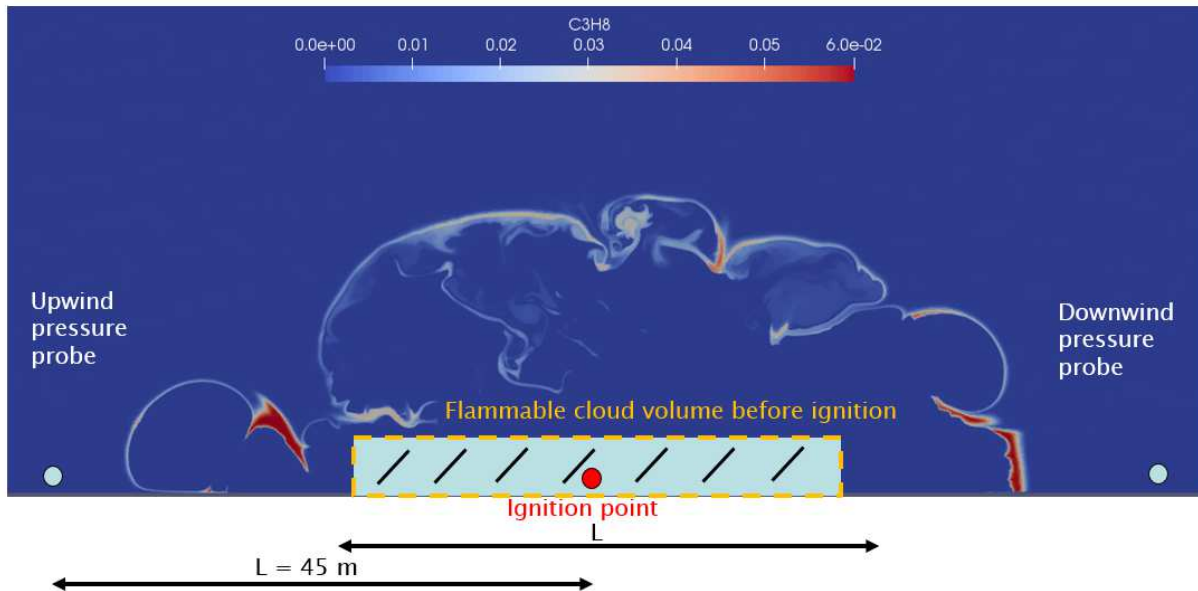


Fig. 3. Location of the pressure probes relative to the flammable cloud and the power plant.

In what follows, a 45 m/s (resp. 55 m/s) flame is a flame propagating with a speed of 45 m/s (resp. 55 m/s) during the hemispherical phase. Computations for a 55 m/s flame propagating in a power plant with either flat or inclined panels show that the far-field pressure effects are higher in the second case (Fig. 4). It tends to confirm that the obstruction and related flame acceleration have a stronger effect on the pressure field than the venting effect between two rows of panels. This result is coherent

with the experimental data of Zeeuwen (1983). A propane/air flame was propagating in a 25 m x 25 m array of regularly spaced vertical tubes with a diameter of 1 m below a full roof. In the array, despite the lack of venting at the roof a maximum pressure of 20 mbar was measured.

Another computation with inclined rows of panels highlights the stronger acceleration (Fig. 5) on a side of the power plant (towards the left in Fig. 3), giving an increase in overpressure about 50 % when compared with the other side.

A 55 m/s flame gives overpressure effects of the same order than a 45 m/s flame when it propagates in inclined rows of panels (Fig. 6). The increase in overpressure is nevertheless about 50 %.

The height of the cloud also plays a role in pressure effects. For half a cloud normally covering the power plant, the far-field pressure peak is about half the pressure peak obtained with a full height cloud (Fig. 7). The venting occurs earlier enabling to reduce pressure effects for the smallest cloud.

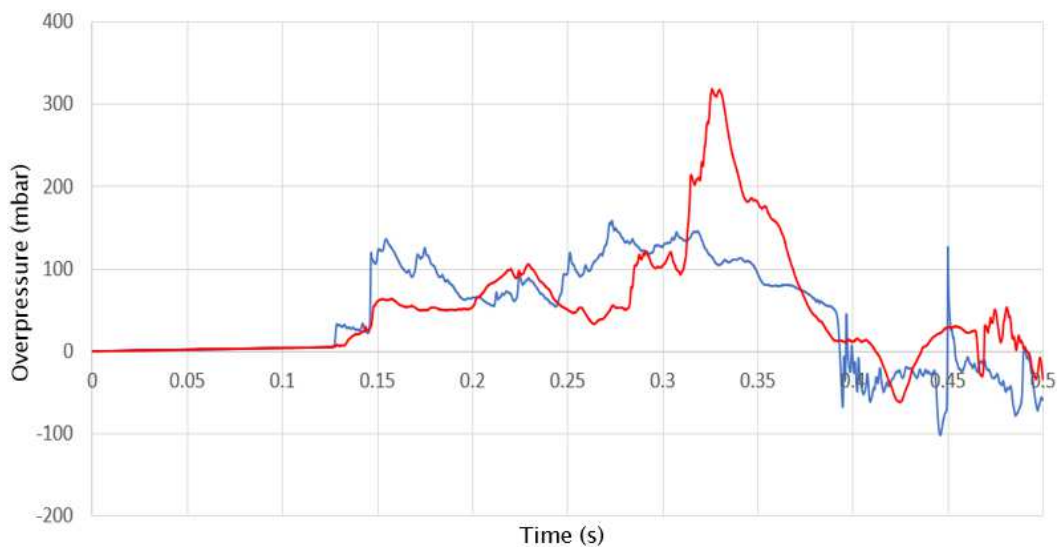


Fig. 4. Overpressure effects 45 m on the left of ignition point. Case of a 55 m/s flame and inclined panels. Blue line: flat panels. Red line: inclined panels.

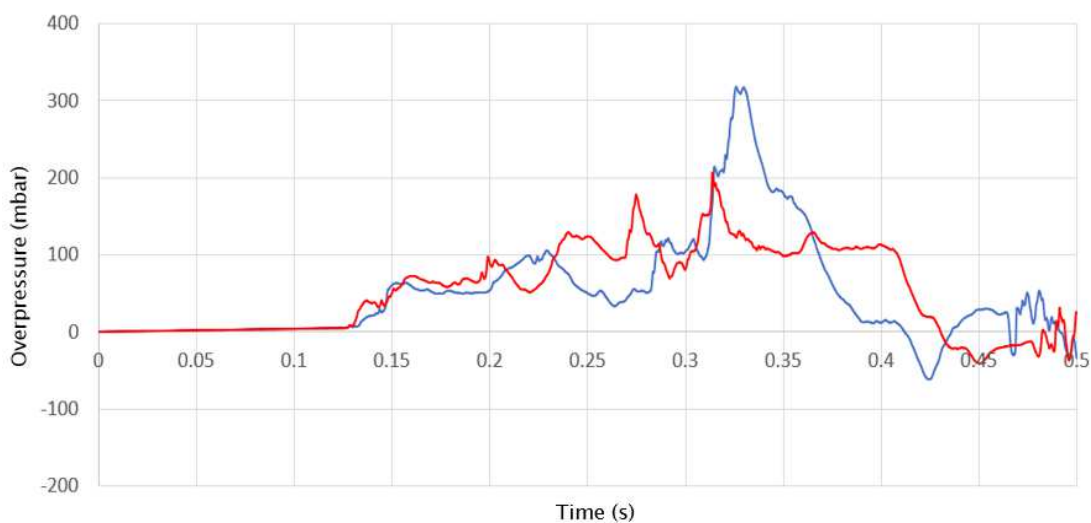


Fig. 5. Overpressure effects on each side of the power plant for a 55 m/s flame. Blue line: upwind pressure probe. Red line: downwind pressure probe.

Finally, the highest far-field effects are obtained in the case of a flammable cloud fully covering the power plant, with inclined panels and a quick flame propagating to the left (see Fig. 3).

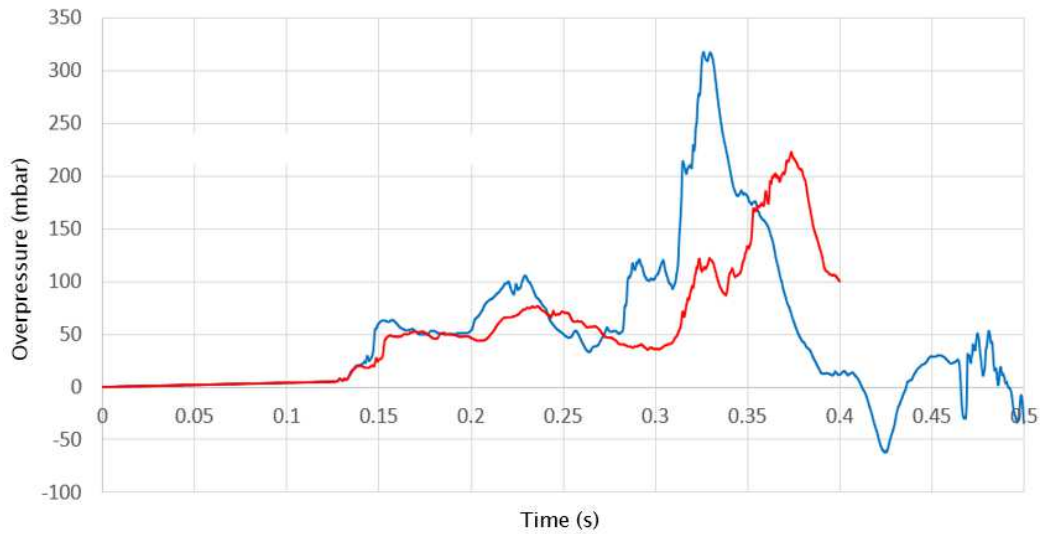


Fig. 6. Overpressure effects 45 m on the left of ignition point. Case of 45 m/s and 55 m/s flames and inclined panels. Blue line: “quick” flame. Red line: “slow” flame.

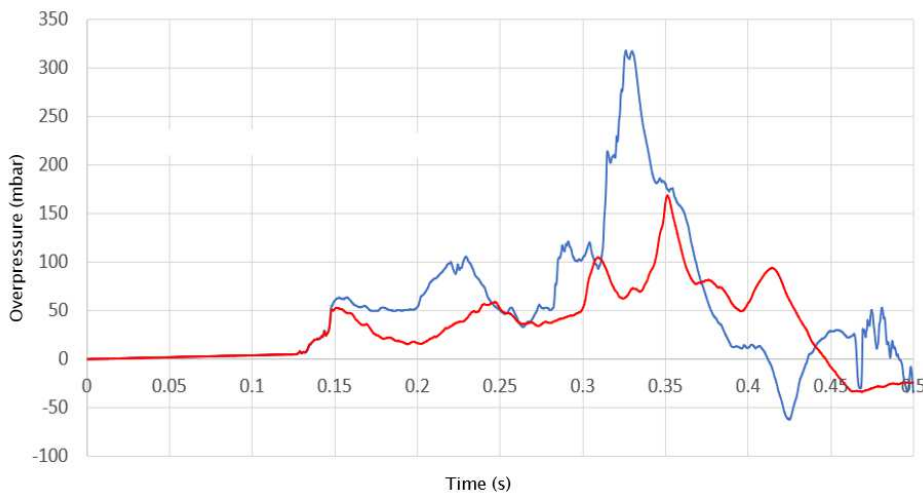


Fig. 7. Overpressure effects 45 m on the left of ignition point. Case of a 55 m/s flame. Blue line: flammable cloud covering the full height of the power plant. Red line: cloud covering half this height.

b. 3D tests and overpressure effects distances

3D CFD computations were finally performed for inclined panels fully covered by a stoichiometric flammable cloud at rest. As mentioned in the beginning of the paper, a first goal was to check if an explosion runaway can occur in the power plant. To do so, the overpressure is computed at a given distance from the side of the flammable cloud. The number of panels is increased from 4 to 6 as well as the size of the flammable cloud to keep all of them covered.

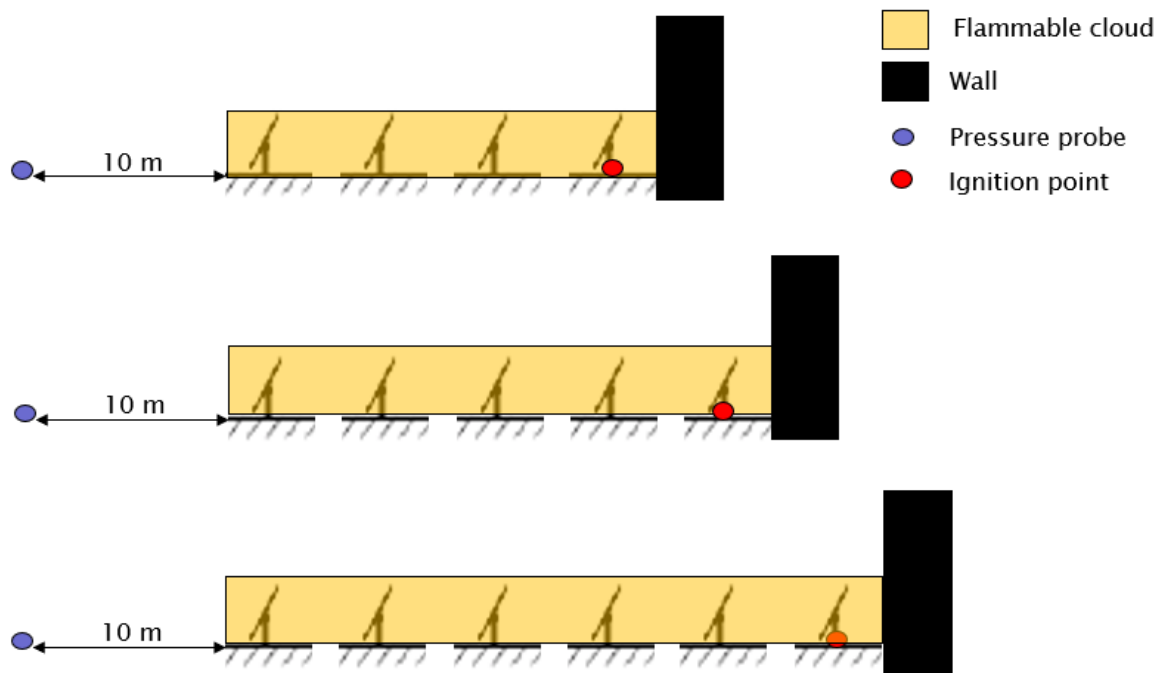


Fig. 8. Principle of the 3D CFD computations. The number of panels the flame interacts with increases from 4 to 6.

The cell width in the zone of interest is 15 cm. A 45 m/s flame representative of propane/air mixture and a 55 m/s flame representative of propylene/air mixture are tested (Fig. 9).

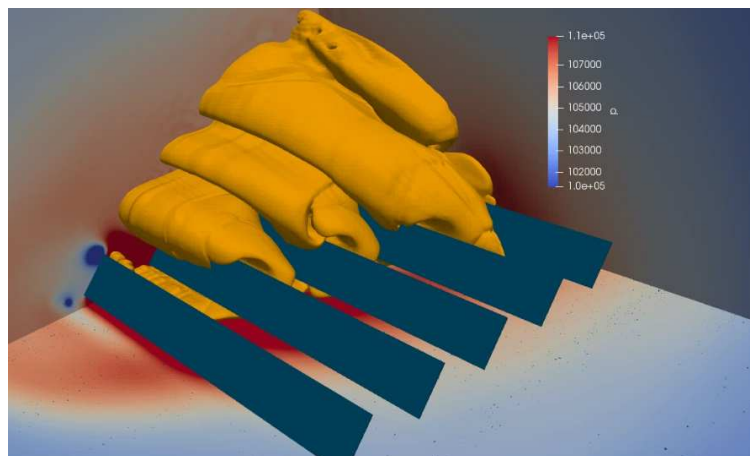


Fig. 9. Example of a CFD result related to flame/solar panels interaction. Shown: pressure fields, flame front (orange), solar panels (dark blue).

The pressure signal computed far from the flammable cloud for the case of the 45 m/s flame are shown in Fig. 10. In all cases, the first pressure peak is related to an interaction of the flame with the two first panels. This first peak is followed by N other pressure peaks where N equals the number of rows minus 2. The final pressure peak which is all the time the highest seems to reach a plateau in terms of magnitude with an increasing number of rows. An explosion runaway can be discarded regarding these aspects.

Almost the same set of characteristic curves is obtained with a 55 m/s flame (Fig. 11). The conclusions just above remain valid.

For both flames, the threshold of 50 mbar is reached about 20 m from the border of the cloud. This distance effect is higher than the one obtained without obstacle. Installing a photovoltaic power plant may have an impact on the regulatory overpressure effects distances but it remains moderate.

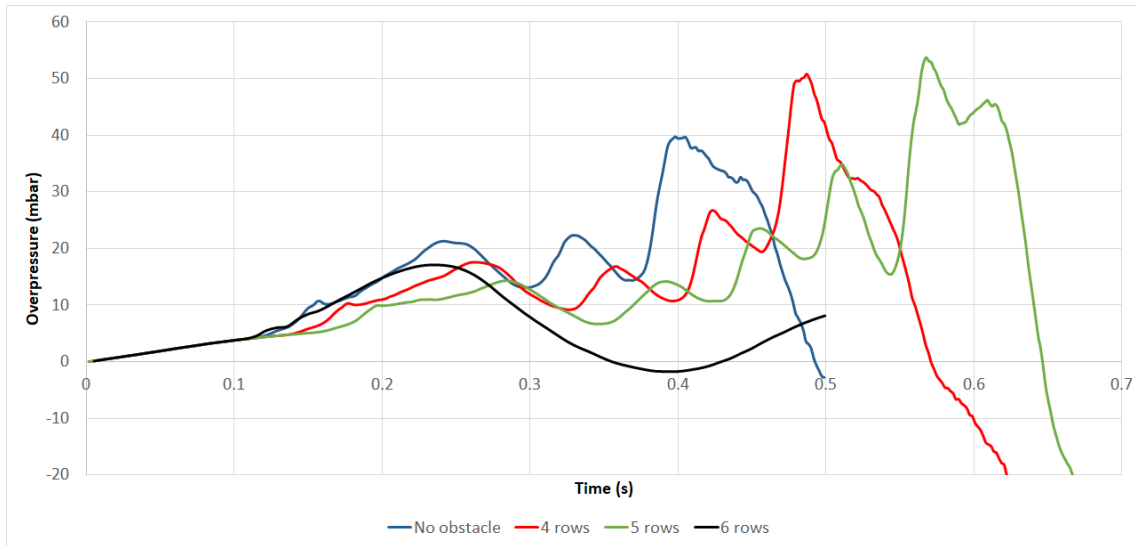


Fig. 10. Computed overpressure 10 m from the flammable cloud border for the cases of no obstacle, 4, 5 and 6 rows of panels in the flammable cloud. Case of the “slow” flame.

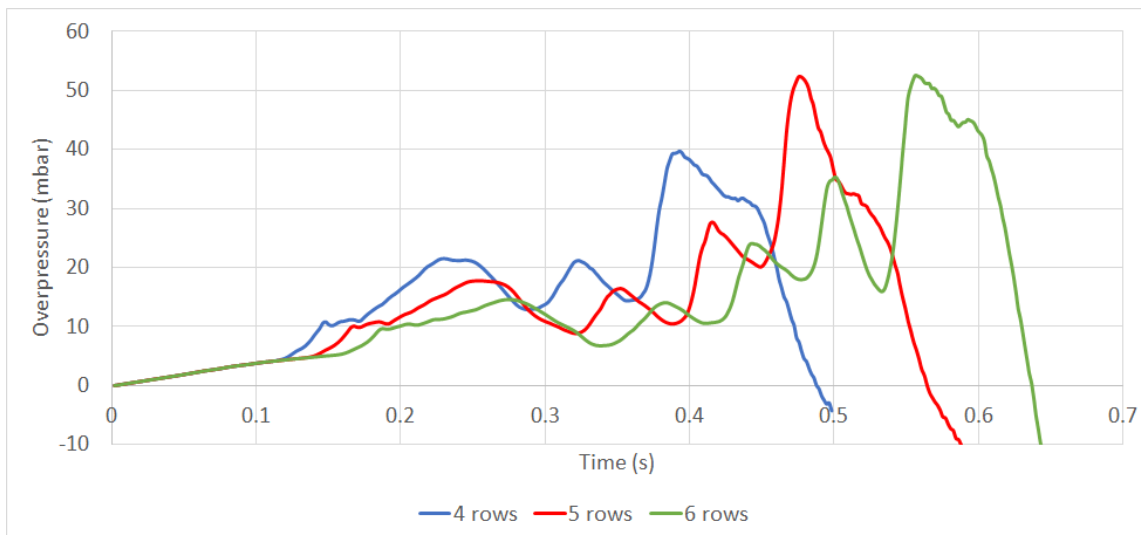


Fig. 11. Computed overpressure 10 m from the flammable cloud border for the cases of no obstacle, 4, 5 and 6 rows of panels in the flammable cloud. Case of the “quick” flame.

5. Conclusions

Total and INERIS worked on the topic of the potentially aggravating effect related to the presence of a photovoltaic power plant in flammable cloud in case of an UVCE. The study was limited to a geometry of a power plant supplied by Total and a flammable cloud formed with hydrocarbons such as propane and propylene.

First FLACS computations showed the pressure effects in the flammable cloud remain below 20 mbar. In order to confirm these results, a method based on phenomenological considerations and CFD was proposed. It appeared with this latter that no explosion runaway occurred for the regarded cases and the maximum distance at which an overpressure of 50 mbar was reached was 20 m from the side of the cloud. Installing a power plant, with the restrictions mentioned in the first paragraph, has an impact when compared to a situation with no obstacle but it remains moderate. These conclusions are globally in line with FLACS simulations, although a bit more restrictive.

References

- Zeeuwen J.P. et al. (1983). Experimental investigation into the blast effect produced by unconfined vapour cloud explosions, *Loss Prevention and Safety Promotion* 4 1, D20
- Van der Berg A.C. et al. (2005). Research to improve guidance on separation distance for the multi-energy method (RIGOS), TNO Prins Maurits Laboratory
- Daubech J. et al. (2016). Les explosions non confinées de gaz et de vapeurs. Omega UVCE. INERIS technical report
- Di Sarli V., Di Benedetto A., Russo G. (2010). Sub-grid scale combustion models for large eddy simulation of unsteady premixed flame propagation around obstacles, *Journal of Hazardous Materials* 180(1-3):71-8
- Quillatre P. (2014). Simulation aux grandes échelles d'explosions en domaine semi-confiné, Thesis Manuscript. University of Toulouse.
- Lecocq, G., Leprette, E., Daubech, J., Proust, C. (2019). Further insight into the gas flame acceleration mechanisms in pipes. Part II: numerical work. *Journal of Loss Prevention in the Process Industries* 62, 103919
- Hansen, O.R., Johnson, D.M. (2010). Improved far-field blast predictions from fast deflagrations, DDTs and detonations of vapour clouds using FLACS CFD, *Journal of Loss Prevention in the Process Industries* 35(15):293-306
- Weller, H.G, Tabor, G. (1998). A tensorial approach to computational continuum mechanics using object-oriented techniques. *Computational Physics*, 12: 620-631.
- Lecocq, G, Richard, S., Colin, O. & Vervisch, L. (2011). Hybrid presumed pdf and flame surface density approaches for Large-Eddy Simulation of premixed turbulent combustion Part 1: Formalism and simulation of a quasi-steady burner, *Combustion and Flame* 158: 1201-1214
- Yang, S. et al. (2018). Role of Darrieus–Landau instability in propagation of expanding turbulent flames. *J. Fluid Mech.* 850, pp. 784-802
- Bauwens, C.R. et al. (2015) Experimental study of spherical-flame acceleration mechanisms in large-scale propane–air flames, *Proc. Combust. Inst.* 35
- Gülder, O.L., Smallwood, G.J. (1995). Inner cut-off scale of flame surface wrinkling in turbulent premixed flames, *Combustion and Flame*, vol. 103, pp. 107-114
- Schneider, H, Pfortner, H. (1983) Fraunhofer-ICT Internal Report: *PNPSicherheitssofortprogramm, Prozeßgasfreisetzung-Explosion in der Gasfabrik und Auswirkungen von Druckwellen auf das Containment*
- Lannoy, A., Leyer J.C., Desbordes D., St Cloud J.P. (1989). *Déflagrations sans turbulence en espace libre : expérimentation et modélisation*, Bulletin de la DER, série A, Electricité de France
- Kostopoulos, D. (2019). *Evaluation des effets de surpression d'un UVCE en présence d'installations photovoltaïques*, Total internal report.